Calculation of mass yields for proton-nucleus spallation reactions

A. Y. Abul-Magd
Max-Planck-Institut für Kernphysik, Heidelberg, Federal Republic of Germany
and Department of Physics, University of Wisconsin, Madison, Wisconsin 53706

W. A. Friedman
Department of Physics, University of Wisconsin, Madison, Wisconsin 53706

J. Hüfner
Institut für Theoretische Physik, Universität Heidelberg, Heidelberg, Federal Republic of Germany
and Max-Planck-Institut für Kernphysik, Heidelberg, Federal Republic of Germany
(Received 10 March 1986)

Nuclear spallation reactions are treated as two step processes involving energy deposition and subsequent evaporation. The first step is calculated in Glauber's multiple scattering formalism with modification for direct knockout processes. Evaporation is treated by following the mean yield of particles from the residual nucleus taken as an excited Fermi gas with ground state provided by the semiempirical mass formula. The spallation mass yield is derived to be an exponential in the mass of the fragments. The amplitude of the exponential and its slope depend on the projectile energy and target mass. Experimental data are well reproduced without free parameters.

I. INTRODUCTION

A high-energy proton penetrates a target nucleus and breaks it. How does it happen? One usually distinguishes three mechanisms: spallation, fission, and multifragmentation (Hüfner[1]). Fragments whose mass number A is larger than $A_T/2$, where A_T is the mass of the target nucleus, are produced by spallation. For heavy target nuclei, fission leads to fragments around $A_T/2$. Light fragments, $10 \lesssim A \lesssim 40$, are said to originate from multifragmentation. The physics of spallation reactions seems well understood: In the first step of the reaction the incident high energy projectile goes through the target nucleus and deposits a significant amount of energy while ejecting only a few nucleons. In the second step the excited nucleus equilibrates, at least partly, and then evaporates nucleons and light nuclei until a particle stable final nucleus, the observed fragment, is formed. The cross section $\sigma(A)$ to produce a fragment with mass A is called the mass yield. It is usually calculated with large numerical effort: An intranuclear cascade circulation is used for the first step while the decay is treated by an evaporation code (see e.g., Bertini *et al.*[2]). Campi *et al.*[3] introduced significant simplifications by applying Glauber's multiple scattering theory to the first step and by treating decay as a diffusion process in the excitation energy and neutron and proton numbers. In this paper we work in the spirit of the approach by Campi *et al.*[3], and succeed in deriving an analytical expression for $\sigma(A)$. The evaluation of the parameters of this expression by simple models provides agreement with experimental data. In this way the dependence of $\sigma(A)$ on the various parameters becomes clear and the physics of spallation very transparent.

II. DISTRIBUTION OF EXCITATION ENERGIES

The first, fast step of the proton-nucleus collision is treated in the spirit of Glauber's multiple scattering theory. This formalism is a good approximation for projectile energies, E_p, above 0.5 GeV. During the collision the projectile proton interacts with ν nucleons of the target nucleus; the cross section σ_ν for these events is given by

$$\sigma_\nu = \int d^2b \frac{T^\nu(b)}{\nu!} e^{-T(b)}, \tag{1}$$

where the thickness function

$$T(b) = \sigma_t^{pN} \int dz\, \rho(b,z) \tag{2}$$

depends on the total proton-nucleon cross section σ_t^{pN} and the density $\rho(\mathbf{x})$ of the target nucleus. The σ_ν are easily calculated numerically for any shape of the nuclear density; some examples are shown in Fig. 1. One observes that the logarithm of σ_ν is well approximated by a linear function ν at least for the large values σ_ν. We therefore write

$$\sigma_\nu = c d^\nu \tag{3}$$

and relate the two constants c and d to more physical quantities, the reaction cross section σ_R and the mean number $\langle \nu \rangle$ of collisions. They are defined as

$$\sigma_R = \sum_{\nu \geq 1} \sigma_\nu = \int d^2b (1 - e^{-T(b)}), \tag{4}$$

$$\langle \nu \rangle = \sigma_R^{-1} \sum_{\nu \geq 1} \nu \sigma_\nu = \frac{A_T \sigma_t^{pN}}{\sigma_R}. \tag{5}$$

With Eq. (3) used in Eqs. (4) and (5) we find

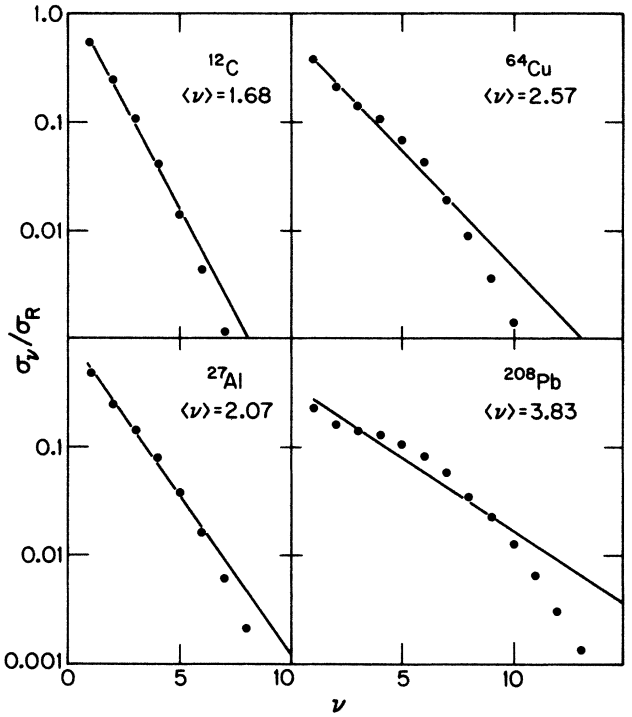

FIG. 1. Cross sections σ_ν for the interaction of the projectile proton with ν target nucleons as a function of ν for several targets. The dots represent the values calculated numerically from Glauber's expression; the solid line is our approximation Eq. (6). Nuclear densities $\rho(r)$ obtained from electron scattering and an elementary cross section of $\sigma_t^{pN}=30$ mb are used for the numerical calculations.

$$\sigma_\nu=\frac{\sigma_R}{\langle\nu\rangle-1}\left[1-\frac{1}{\langle\nu\rangle}\right]^\nu . \tag{6}$$

This approximate formula is compared with the exact values in Fig. 1 and reproduces them well over nearly two orders of magnitude. We have not been able to drive the formula Eq. (6) from the defining Eq. (1).

In each collision between the projectile and a target nucleon an energy E is transferred from the projectile to a target nucleon, and via equilibration also to the entire target nucleus. We denote by $F_1(E)$ the distribution of energy E transferred to one target nucleon and assume it to be normalized,

$$\int_0^\infty dE\,F_1(E)=1 . \tag{7}$$

Guided by the fact that the elastic nucleon-nucleon cross section at high-energies behaves like

$$\frac{d\sigma}{d\Omega}=\sigma_0 e^{-bq^2}, \tag{8}$$

where q is the momentum transfer and $q^2/2m=E$ the transferred energy, we choose an exponential shape

$$F_1(E)=(1/E_0)\exp(-E/E_0) . \tag{9}$$

We also use this form for projectile energies E_p above the first inelastic threshold in nucleon-nucleon scattering, where energy is also deposited into the nucleus by inelastic processes. The dependence of the parameter E_0 in Eq. (9) on E_p will be discussed below.

If the projectile collides with ν target nucleons independently, the distribution $F_\nu(E)$ of deposited energy is obtained by folding $F_1(E)$ ν times, which provides

$$F_\nu(E)=\frac{1}{(\nu-1)!}(E^{\nu-1}/E_0^\nu)\exp(-E/E_0) . \tag{10}$$

This formula is exact only if E_0 is independent of E_p. Since the projectile slows down during the passage through the target nucleus, E_p decreases. We suggest below a procedure for evaluating E_0 for cases in which E_0 depends strongly on the instantaneous projectile energy.

The cross section $d\sigma/dE^*$ to deposit a certain amount of energy E^* into the nucleus is a superposition of events with different numbers of collisions, ν; therefore

$$\frac{d\sigma}{dE^*}=\sum_{\nu\geq 1}\sigma_\nu F_\nu(E^*) . \tag{11}$$

This sum can be evaluated analytically for the σ_ν given in Eq. (6) and the F_ν given in Eq. (10). One finds

$$\frac{d\sigma}{dE^*}=\frac{\sigma_R}{\langle\nu\rangle E_0}\exp\left[-\frac{E^*}{\langle\nu\rangle E_0}\right] . \tag{12}$$

This result is very simple: Independent of how large the target nucleus is, the energy distribution is always an exponential.

The mean energy deposited is given by $\langle\nu\rangle E_0$, which is the average energy deposited in reactions for which the number of collisions takes the mean value, $\langle\nu\rangle$. To this point we have ignored the possibility that some collisions end with the knockout of the target nucleons and hence provide no substantial energy to the residual nucleus. The mean energy deposited should thus be modified to account for the direct knockout collisions. This can be accomplished by replacing $\langle\nu\rangle E_0$ in Eq. (12) by $\langle\nu\rangle(1-f)E_0$, where f is the fraction of all collisions that lead to direct knockout.

We now estimate the value of f by regarding the nucleus as a uniform sphere of radius R in which the nucleons have a mean path λ. Guided by the fact that the momentum transferred to the target nucleons will be perpendicular to the beam directions (z), we divide the sphere into two regions, the boundaries of which are indicated in Fig. 2. The inner boundary is generated by rotating about the z axis an arc achieved by shifting downward a distance λ the circumference of a circle of radius of R originally centered at the origin. Target nucleons in the inner region must travel a distance λ or greater to get out and hence are assumed not to participate in direct knockout reactions. On the other hand, half of the collisions in the outer region, those for which the resulting momentum transfer is toward the surface, are assumed to lead to knockout. The ratio of the volume of the outer region to that of the entire sphere is found to be $\frac{3}{2}(\lambda/R)$ plus terms of order $(\lambda/R)^2$. Accordingly the estimated fraction of collisions leading to direct knockout is

$$f\cong\tfrac{1}{2}\,\tfrac{3}{2}\lambda/R=\tfrac{3}{4}\lambda/R . \tag{13}$$

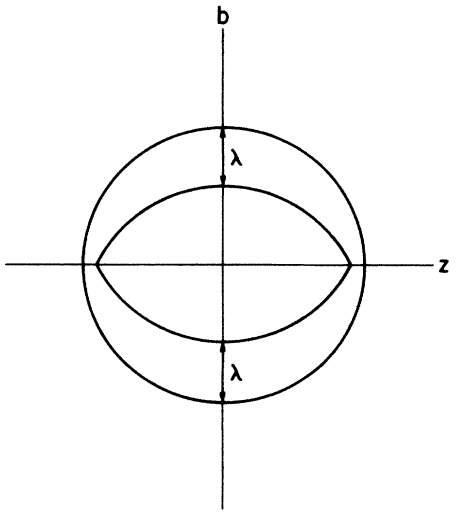

FIG. 2. Schematic division of the nucleus into an outer "knockout" and inner "spallation" regions.

It is easily shown that for a uniform sphere

$$\langle \nu \rangle = \tfrac{4}{3} R/\lambda \tag{14}$$

and thus we take

$$f = 1/\langle \nu \rangle , \tag{15}$$

leading to the following modified form of Eq. (12):

$$\frac{d\sigma}{dE^*} = \frac{\sigma_R}{(\langle \nu \rangle - 1)E_0} \exp\left[-\frac{E^*}{(\langle \nu \rangle - 1)E_0} \right] . \tag{16}$$

We next calculate the single-collision slope parameter E_0 and its dependence on the projectile energy E_p: $E_0(E_p)$. According to Eq. (9), E_0 is the mean energy which is transferred in a proton-nucleon collision. For energies below the first inelastic threshold, the energy transferred in an elastic collision is

$$E_0^{\rm el} = \int_0^{p/\sqrt{2}} (q^2/2m) \frac{d^2\sigma}{dq^2} d^2q \Big/ \int_0^{p/\sqrt{2}} \frac{d^2\sigma}{dq^2} d^2q . \tag{17}$$

The upper limit, $p/\sqrt{2}$, where p is the laboratory momentum of the projectile, is introduced by defining the faster nucleon after the collision to be the projectile which proceeds to the next collision and the slower one to stay inside the target nucleus. Using Eq. (8) in Eq. (17) one finds

$$E_0^{\rm el} = \frac{1}{2mb} \left\{ 1 - \frac{p^2 b}{2} \left[\exp\left[\frac{p^2 b}{2} \right] - 1 \right]^{-1} \right\} , \tag{18}$$

which has the limits

$$E_0^{\rm el} \sim E_p/4 \text{ for } E_p \lesssim 0.5 \text{ GeV}$$
$$\sim \tfrac{1}{2} mb \text{ for } E_p \gtrsim 2 \text{ GeV} . \tag{19}$$

The slope parameters b for elastic NN scattering are well determined (e.g., Igo[4]), and may be parametrized by

$$b(E_p) = 0; \quad E_p \lesssim 0.28 \text{ GeV}$$
$$= 8\sqrt{(1 - 0.28/E_p)}\ (\text{GeV}/c)^{-2};$$
$$0.28 \text{ GeV} \lesssim E_p \lesssim 10 \text{ GeV} . \tag{20}$$

Typical values for the mean energy $E_0^{\rm el}$ lie between 50 and 100 MeV.

We proceed to estimate the energy deposition due to inelastic proton-nucleus collisions. The formation of an intermediate Δ resonance is the dominant mechanism for pion production from the inelastic threshold for $pN \rightarrow NN\pi$ up to projectile energies E_p of several GeV. The decay of the Δ resonance is an additional source for energy deposition in p-nucleus collisions. We take this effect into account by writing the mean deposited energy as a sum of two terms,

$$E_0 = E_0^{\rm el} + \frac{\sigma_{\rm in}^{pN}}{\sigma_t^{pN}} \frac{m_\Delta - m}{2} , \tag{21}$$

where m_Δ is the mass of the Δ resonance. The factor $\frac{1}{2}$ reflects our assumption that only the slow Δ (i.e., when a *target* nucleon is excited to a Δ) deposits its energy into the target nucleus, while a fast Δ decays outside the nucleus.

While traversing the nucleus, the projectile loses energy. Since E_0 depends on the projectile energy, the *mean* deposited energy per collision changes during the traversal of the nucleus. If one takes this effect into account exactly one loses the simplicity of the formula Eq. (10). We take this effect into account approximately by using the mean value $\overline{E_p}$ rather than the initial value E_p in evaluating E_0. To find $\overline{E_p}$ we average over the degradation process from the initial proton energy E_p to its final energy E_f:

$$\overline{E}_p = \int_{E_p}^{E_f} E \left[\frac{dE}{dN} \right]^{-1} dE \Big/ \int_{E_p}^{E_f} \left[\frac{dE}{dN} \right]^{-1} dE , \tag{22}$$

where dE/dN is the energy change per collision, and we take

$$\frac{dE}{dN} \cong -E_0(E) , \tag{23}$$

with $E_0(E)$ given by Eq. (21). The final energy E_f is determined by

$$\langle \nu \rangle = \int_{E_p}^{E_f} \left[\frac{dE}{dN} \right]^{-1} dE . \tag{24}$$

for example, with $E_p < 0.5$ GeV, we find from Eqs. (22)–(24)

$$E_0(\overline{E}_p) \cong \frac{E_p}{\langle \nu \rangle} (1 - e^{-\langle \nu \rangle/4}) . \tag{25}$$

In this section we have derived the distribution $d\sigma/dE^*$ of energy E^* which is deposited into a target nucleus. Clearly, Eq. (16) and the subsequent expressions for E_0 involve approximations in several respects. In order to gain some confidence in their reliability we compare the predictions of Eq. (16), using Eq. (25), with the

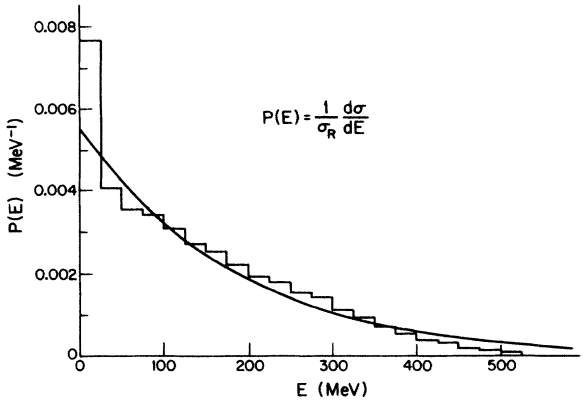

FIG. 3. The distribution of excitation energy E^* in proton-^{159}Tb collisions at $E_p=600$ MeV. The histogram is the result of an intranuclear cascade calculation by Bertini *et al.* (Ref. 2), the solid line is our analytical result, Eq. (16).

results of an intranuclear cascade calculation. Figure 3 shows this comparison. The agreement is quite satisfactory, except for excitation energies close to the E_p.

III. THE MASS YIELD CURVE

After the first, fast step of the reaction, the target nucleus is in a state of high excitation energy. It also has lost a few nucleons which have been ejected during the cascade. Since their number is small compared to the target mass A_T, we neglect them. Thus after the first step of the reaction, the target nuclei present are an ensemble of nuclei with mass A_T and a distribution of excitation energies characterized by $d\sigma/dE^*$. A nucleus with a given excitation energy emits nucleons or light nuclei until a particle stable final fragment with mass $A\ (=A_T-\Delta A)$ is reached. The ratio,

$$\epsilon=\frac{\Delta E^*}{\Delta A}, \tag{26}$$

of excitation energy ΔE^* carried away by ΔA emitted nucleons is the crucial parameter which relates the mass yield curve to the distribution of excitation energies. If we assume that ϵ is independent of E^* and A, i.e., ϵ is the same at each step of the evaporation chain, then the mass yield has been derived by Campi *et al.*[3] to be

$$\sigma(A)=\epsilon\left.\frac{d\sigma}{dE^*}\right|_{E^*=(A_T-A)\epsilon}. \tag{27}$$

When this relation is combined with the formula for $d\sigma/dE$, Eq. (16), we obtain

$$\sigma(A)=\sigma_R\frac{\epsilon}{(\langle\nu\rangle-1)E_0}\exp\left[-\frac{\epsilon}{(\langle\nu\rangle-1)E_0}(A_T-A)\right]. \tag{28}$$

This result has an amazingly simple form. The shape of $\sigma(A)$ is an exponential in the mass A of the fragment. The slope s of the exponential is a dimensionless parameter

$$s(A_T,E_p)=\frac{\epsilon}{(\langle\nu\rangle-1)E_0} \tag{29}$$

which depends on A_T and E_p since the two quantities, ϵ and $\langle\nu\rangle$ depend on A_T, while $\langle\nu\rangle$ and E_0 depend on E_p.

We next discuss the magnitude of the parameter ϵ and its dependence on the target mass. To begin with we consider reactions for which the mass loss is all borne by neutrons, since there are extensive data on (heavy ion, xn) reactions. In order to determine the mean number of evaporated neutrons we shall estimate the mean kinetic energy E_k and the mean separation energy for the emitted neutrons. For the former we use a Fermi gas model to describe the excited nucleus, while for the latter we use the semiempirical mass formula for ground state energies.

In calculating the mean kinetic energy E_k we assume that the spectrum of neutrons at any temperature is provided by

$$\frac{dn}{dE_k}\propto E_k\exp(-E_k/T), \tag{30}$$

so that the mean kinetic energy is given by $\langle E_k\rangle=2T$. During the course of the evaporation process the temperature decreases towards zero from an initial value T_{max}. We must calculate the average temperature T_{av}, during the evaporation process. This is straightforward as long as T_{max} is much less than the average neutron binding energy.

The value of T_{av} is defined by

$$T_{av}=\int_{T_{max}}^{0}T\,dN\Big/\int_{T_{max}}^{0}dN, \tag{31}$$

where dN is the differential of the neutron yield. Introducing the average binding energy $\langle B\rangle$ we have

$$dN\cong-\frac{1}{2T+\langle B\rangle}dE^*. \tag{32}$$

With the excitation energy given by $E^*=aT^2$, where a is the Fermi-gas density parameter (taken between $A/12$ and $A/8$), we obtain

$$dN\cong-\frac{2aT}{2T+\langle B\rangle}dT\cong\frac{2aT}{\langle B\rangle}\left[1-\frac{2T}{\langle B\rangle}\right]dT. \tag{33}$$

Using Eq. (33) in Eq. (31) we find (to lowest order in $T_{max}/\langle B\rangle$):

$$T_{av}=\tfrac{2}{3}T_{max}\left[1+\frac{1}{6}\frac{T_{max}}{\langle B\rangle}\right]. \tag{34}$$

Finally with $T_{max}=(E^*/a)^{1/2}$ we obtain the mean kinetic energy

$$\langle E_k\rangle=\tfrac{4}{3}(E^*/a)^{1/2}\left[1+\tfrac{1}{6}(E^*/a)^{1/2}\frac{1}{\langle B\rangle}\right]. \tag{35}$$

In order to calculate the mean binding energy $\langle B\rangle$ we use the semiempirical mass formula neglecting the pairing and shell corrections. (These corrections are not expected to play an important role at the high excitation energies involved in the present study.) We therefore assume that the mass defect for the decaying nucleus is given by

$$M(Z,A)=a_v A-a_s A^{2/3}-a_c Z^2/A^{1/3} - a_a(A-2Z)^2/A\,, \tag{36}$$

with[5] $a_v=14.1$ MeV, $a_s=13.0$ MeV, $a_c=0.595$ MeV, and $a_a=19.0$ MeV. The binding energy of N neutrons removed from a nucleus of mass A and change Z is given by $[M(Z,A)-M(Z,A-N)]$. This difference may be expanded in powers of N:

$$M(Z,A)-M(Z,A-N)=N\frac{\partial M(Z,A)}{\partial A}-\tfrac{1}{2}N^2\frac{\partial^2 M(Z,A)}{\partial A^2} + \cdots\,. \tag{37}$$

Neglecting terms higher than second order we obtain $\langle B\rangle$:

$$\langle B\rangle \cong \frac{\partial M}{\partial A}-\tfrac{1}{2}N\frac{\partial^2 M}{\partial A^2}\,. \tag{38}$$

To find the binding energy for the $(N+1)$th neutron B_{N+1} we use similar arguments to obtain

$$B_{N+1}=\frac{\partial M}{\partial A}-N\frac{\partial^2 M}{\partial A^2}\,. \tag{39}$$

Finally, to find the mean number N of neutrons emitted in a given reaction, we divide the available excitation energy by the average energy carried by each removed neutron. We assume the energy available is E^*-B_{N+1}, taking into consideration the threshold energy for neutron emission. Then we obtain N from

$$N=\frac{E^*-B_{N+1}}{\langle E_k\rangle+\langle B\rangle}\,, \tag{40}$$

and using Eqs. (38) and (39),

$$N=\left[E^*-\frac{\partial M}{\partial A}+N\frac{\partial^2 M}{\partial A^2}\right]\Big/\left[\langle E_k\rangle+\frac{\partial M}{\partial A}-\tfrac{1}{2}N\frac{\partial^2 M}{\partial A^2}\right], \tag{41}$$

which may be solved for N.

We have used the result of Eq. (41) to calculate the mean number of neutrons emitted by the nuclei ^{142}Ce, ^{211}Po, ^{205}At, and ^{204}Po as functions of the excitation energies. In Fig. 4 these calculated values are compared with the positions of the peaks of the experimental excitation functions for the reactions ^{130}Te(^{12}C,xn), ^{197}Au(^{14}N,xn), ^{185}Re(^{20}Ne,xn), and ^{164}Dy(^{40}Ar,xn) taken from a compilation by Neubert.[6] The level density parameter used in determining $\langle E_k\rangle$ is taken equal to $A/12$ MeV^{-1} (the solid curves) and $A/8$ MeV^{-1} (the dashed curves). The agreement between calculation and experiment is good. The uncertainty in the determination of the peak positions makes inconclusive any definite preference for one density parameter over the other.

We have also used Eq. (41) to examine the dependence on the compound-nucleus mass of the ratio of excitation energy to the number of neutrons emitted, E^*/x, in a (HI,xn) reaction. For this study we assumed the target to have charge related to mass by the conditions providing the valley of stability in the mass formula of Eq. (37). The projectile ion then determines the mass and charge for the resulting compound nucleus. In Fig. 5 we show the results E^*/x for two different projectiles using Fermi gas density parameters of $A/8$ and $A/12$ MeV^{-1} for comparison. Calculated results are shown for two values of excitation energy -50 and 150 MeV which represent the approximate range of excitation energy for the experimental data shown. The sensitivity to projectile, and consequently the isospin of the compound nucleus, is extremely weak. There is some sensitivity to the value of the gas density constant, but no clear preference is evident. The largest sensitivity is related to the change in the

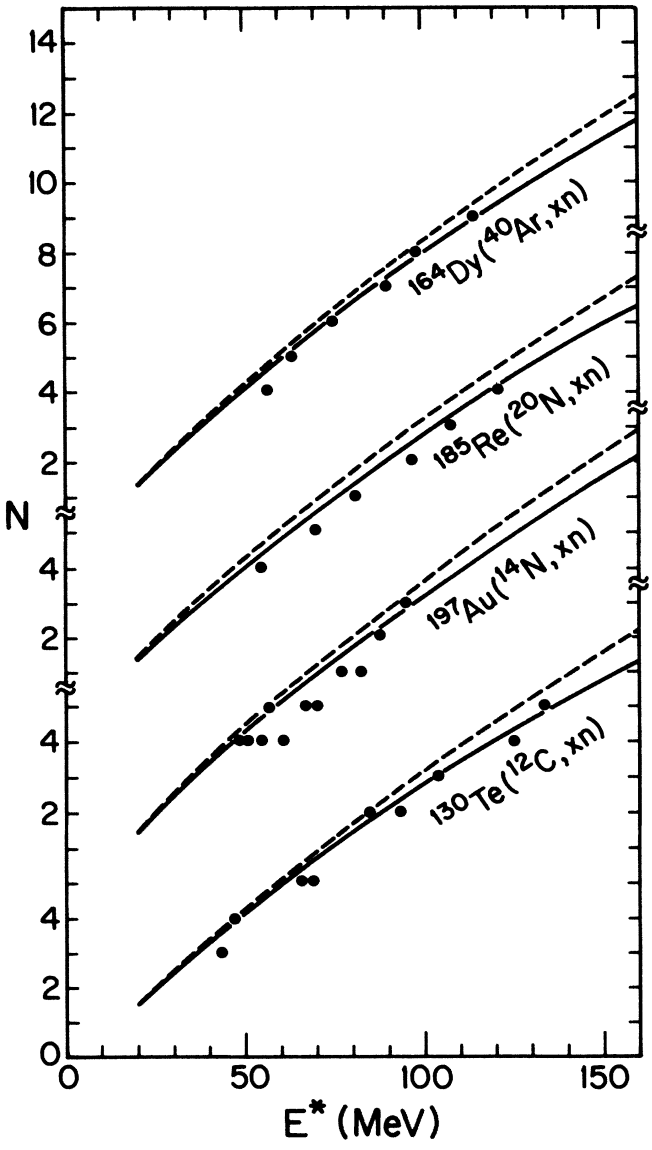

FIG. 4. The mean number N of neutrons emitted by the compound nuclei ^{142}Ce, ^{211}P$_0$, ^{205}At, and ^{204}P$_0$ as functions of excitation energy. The experimental points are taken from Neubert's compilation (Ref. 6) of the peaks of (HI,xn) reactions. The solid curves are calculated from Eq. (40) and correspond to a choice of $a=A/12$ MeV^{-1} for the level density parameter while the dashed curves correspond to $a=A/8$ MeV^{-1}.

excitation energy. This variation, however, is small when compared to the experimental deviation for the quantity E^*/x for each mass (shown by the error bars).

Encouraged by the good agreement between the simple model and the data for the (HI,xn) reactions, we have used the evaporation model of Friedman and Lynch[7] to estimate general mass loss for heated nuclei. This model incorporates precisely the same Fermi-gas and semiempirical mass formula, features discussed above for the HI-xn reactions, but allows for the emission of charged particles and more massive particles in addition to neutrons. We have used this model to calculate the loss of mass ΔA, for given excitation energies and nuclei. Specifically we have studied ^{64}Cu, ^{108}Ay, and ^{197}Au. In Fig. 6 we show the calculated value of $\Delta E^*/\Delta A$ [or the parameter ϵ of Eq. (26)] as a function of initial excitation energy. Two values of a, $A/8$ and $A/12$, were used for comparison. We find ϵ slowly varying with the excitation energy, thus justifying Eq. (27).

In addition, we can take specific values of ϵ from the curves in Fig. 6 in order to evaluate Eq. (28) for direct comparison with experimental spallation mass yields presented below. Having obtained an estimate of the parameter ϵ we next examine the energy dependence of the slope parameter $s(E_p,A_T)$ given in Eq. (29) as a function of incident energy. This dependence has been extracted

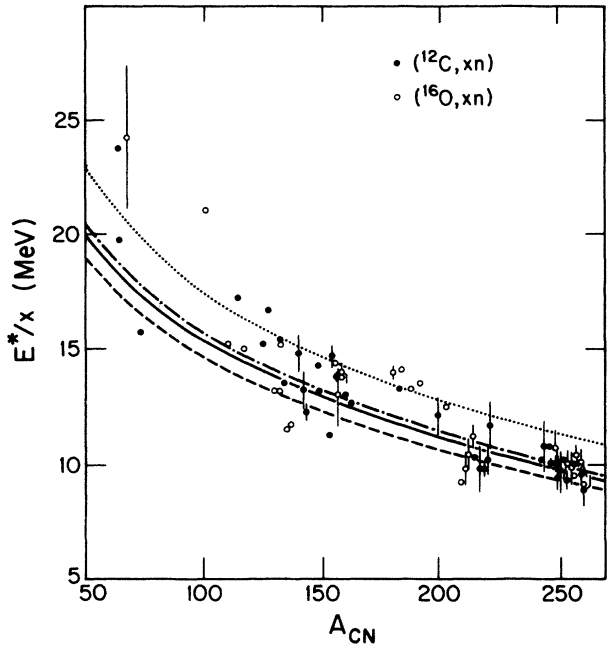

FIG. 5. The loss of excitation energy ϵ per emitted neutron from the excitation function in heavy ion reactions of the type A_T(HI,xn), Eq. (26), as a function of the mass of the compound nucleus. The data points have been prepared from a compilation by Neubert (Ref. 6). The closed circles are for carbon and the open ones for oxygen as projectiles. The calculations are indicated by the following curves: solid for (^{12}C,$a=A/12$ MeV^{-1},$E^*=50$ MeV); dashed-dotted for (^{16}O,$a=A/12$ MeV^{-1},$E^*=50$ MeV); long-dashed for (^{12}C,$a=A/8$ MeV^{-1},$E^*=50$ MeV); short-dotted for (^{16}O,$a=A/12$ MeV^{-1},$E^*=150$ MeV).

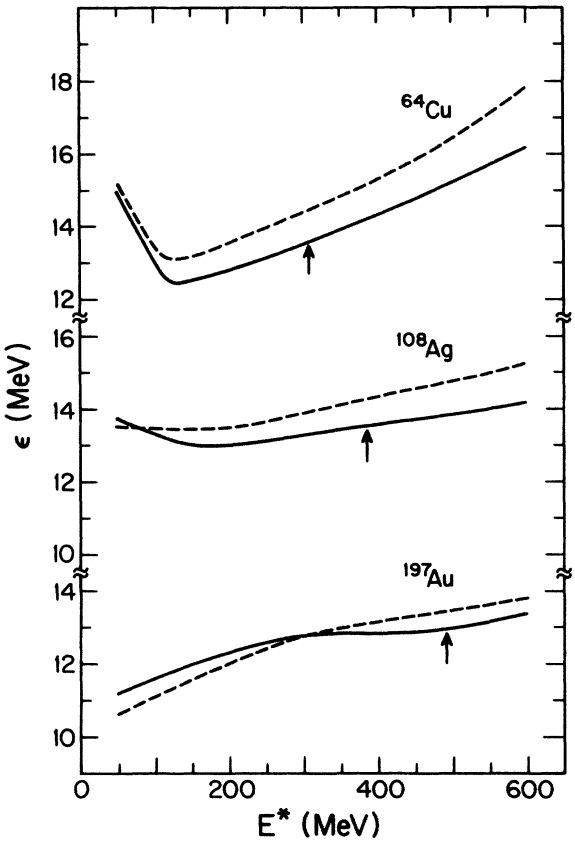

FIG. 6. The excitation energy removed per unit mass evaporation as a function of excitation energy for the compound nuclei ^{64}Cu, ^{109}Ag, and ^{197}Au. The solid curves correspond to $a=A/12$ MeV^{-1} and the dashed to $a=A/8$ MeV^{-1}. The arrows indicate the energies used for calculations described in the text.

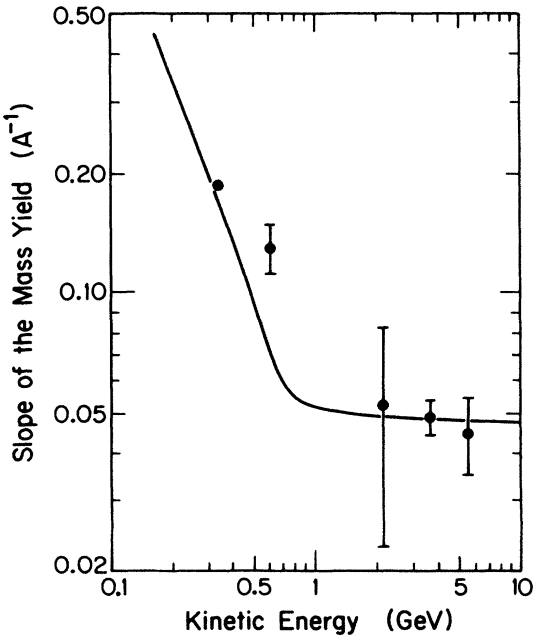

FIG. 7. The slope $s(E_p)$ of the mass yield curve as a function of the projectile energy E_p for p-Cu collisions. The data points are taken from Cumming *et al.* (Ref. 11).

from data for p-Cu reactions over a wide range of energies. We compare the prediction of Eq. (29) with these data. We evaluated $\langle \nu \rangle$ from Eq. (5) assuming the effective NN cross section in nuclear matter is well represented by[8]

$$\bar{\sigma}_t^{\mathrm{pN}} = \left[1 - \frac{7}{5}\frac{E_F}{E}\right](Z\sigma_t^{\mathrm{pp}} + N\sigma_t^{\mathrm{pn}})/A\,, \tag{42}$$

where E_F is the Fermi energy. The experimental nucleon-nucleon cross sections are taken from Ref. 9. The total reaction cross section for Cu is taken from the measurement by Renberg *et al.*[10]

Figure 6 provides an estimate of ϵ, and E_0 ($\bar{E}_p$) is evaluated according to Eqs. (18), (21), and (22). The resulting values for the slope of the mass yield as a function of energy for interactions of protons with copper[11] are shown in Fig. 7. The model is in excellent agreement with the data. We have limited the comparison to energies less than 5 GeV, above which energy the mechanism of Δ production ceases to be dominant.

Finally in Fig. 8 we directly compare the prediction of Eq. (28) with experimental[12–14] spallation mass yields from 3 GeV protons interacting with Cu, Ag, and Au. The theoretical results which contain no adjustable parameters reproduce the experimental points in trend and magnitude.

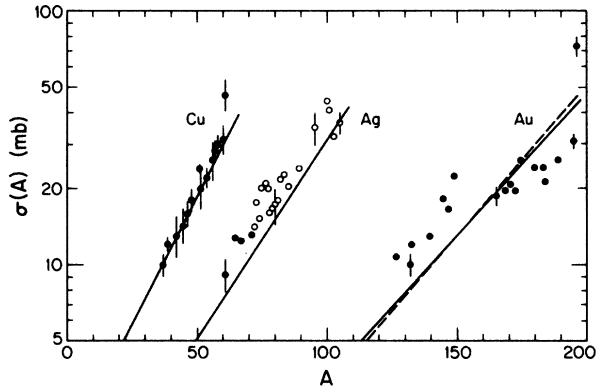

FIG. 8. Data and calculation for the mass yield curves for proton nucleus spallation reactions. The data are for 3 GeV protons on Cu [by Cumming *et al.* (Ref. 12)], Hg [Katcoff *et al.* (Ref. 13)], and Au [Kaufman *et al.* (Ref. 14)].

IV. SUMMARY AND CONCLUSIONS

As early as 1966 Rudstam[15] proposed to parametrize the mass yield curve for spallation products by an exponential,

$$\sigma(A) = \sigma_0 \exp(PA)\,, \tag{43}$$

where σ_0 and P were empirical parameters which depend on the projectile energy E_p and the mass A_T of the target nucleus. In this paper we are able to *derive* the shape Eq. (43) from multiple scattering and an approximation to the evaporation chain. Explicit expressions are given for the parameters P and σ_0:

$$P = s(A_T, E_p) = \frac{\epsilon}{(\langle \nu \rangle - 1)E_0}\,,$$
$$\sigma_0 = \sigma_R P e^{-PA_T}\,, \tag{44}$$

where $\langle \nu \rangle$ is the mean number of proton-nucleon collisions in a given target nucleus, E_0 the mean energy which is transferred to the target nucleus in one proton-nucleon collision, and ϵ is the average energy carried away by one evaporated nucleon. Since Eq. (43) with the parameters calculated by Eq. (44) reproduces the data in magnitude and trend, one may say without arrogance that proton-induced spallation reactions are quantitatively understood. They are two-step processes, excitation of the target and subsequent evaporation.

ACKNOWLEDGMENTS

The authors thank J. Aichelin, X. Campi, and K. Werner for several discussions. One of us (J.H.) wishes to acknowledge support in part by a grant from the Gesellschaft für Schwereionenforschung (GSI), Darmstadt, and one of us (W.A.F) wishes to acknowledge support in part by the U.S. National Science Foundation.

[1] J. Hüfner, Phys. Rep. **125**, 129 (1985).
[2] H. W. Bertini, A. H. Culkowski, O. W. Hermann, N. B. Gove, and M. P. Guthrie, Phys. Rev. C **17**, 1382 (1978).
[3] X. Campi and J. Hüfner, Phys. Rev. C **24**, 2199 (1981).
[4] G. J. Igo, Rev. Mod. Phys. **50**, 523 (1978).
[5] P. Marmier and E. Sheldon, *Physics of Nuclei and Particles* (Academic, New York 1969), Vol. 1.
[6] W. Neubert, Nucl. Data Tables **11**, 531 (1973).
[7] W. A. Friedman and W. G. Lynch, Phys. Rev. C **28**, 16 (1983).
[8] L. Goldberger, Phys. Rev. **74**, 1269 (1948).
[9] L. Ray, Phys. Rev. C **20**, 1878 (1979).
[10] P. U. Renberg, D. F. Measday, M. Pepin, P. Schwaller, B. Favier, and C. Richard-Serre, Nucl. Phys. **A183**, 81 (1972).
[11] J. B. Cumming, P. E. Haustein, T. J. Ruth, and G. J. Virtes, Phys. Rev. C **17**, 1632 (1978).
[12] J. B. Cumming, P. E. Haustein, R. W Stoenner, L. Mausner, and R. A. Naumann, Phys. Rev. C **10**, 739 (1974).
[13] S. Katcoff, H. R. Fickel, and A. Wyttenbach, Phys. Rev. **166**, 1167 (1968).
[14] S. B. Kaufman and E. P. Steinberg, Phys. Rev. C **22**, 167 (1980).
[15] G. Rudstam, Z. Naturforsch. **21a**, 1077 (1966).